Geological Survey of Canada
Open File 7895

REACTIVATED FAULT SYSTEMS AND THEIR EFFECTS ON OUTCROP PATTERNS OF THIN-SKINNED EARLY THRUST IMBRICATIONS IN THE KIGGAVIK URANIUM CAMP, NUNAVUT

A. Anand[1] and C.W. Jefferson[1]

ABSTRACT

Reactivated ENE-WSW-trending dextral fault arrays in the northeast Thelon Basin region are exemplified by the dextral, north-down, oblique-slip Thelon and Judge Sissons faults. We compiled and interpreted a variety of geoscience data, including lineaments, detailed outcrop and samples to produce new maps that incorporate past observations by Industry and academic studies. The reactivated fault arrays discordantly transect the main basement foliation and comprise zones of sub-parallel brittle and ductile fractures detailed here and interpreted as products of Riedel shear systems that were successively reactivated by multiple tectonic events with varying principle stresses.

The key basement assemblage dismembered by the fault systems is a thrust- and fold-imbricated complex (hereafter "imbricate complex") comprising 2.6 Ga epiclastic rocks and rhyolite of the Pukiq Lake formation (Snow Island Suite), and Paleoproterozoic quartzite of the Ketyet River group. The imbricate complex structurally overlies and may include some metagreywacke of the Neoarchean Pipedream assemblage, Woodburn Lake group, from west of Judge Sissons Lake to southeastern Schultz Lake, trending through the Andrew Lake, End, Granite Grid, Bong and Kiggavik uranium deposits. It lies between two inferred low-angle structures: Granite Thrust to the W and the Pukiq discontinuity to the SE. These are in turn offset by the Thelon and Judge Sissons faults. Imbrication took place during DP1. The much younger Thelon Basin developed trans-extensionally during DP6-DP7 (Table 1).

Intersections between reactivated brittle-ductile fractures and the imbricate complex likely created conduits and barriers to hydrothermal fluid flow forming basement-hosted uranium deposits during and/or after filling of Thelon Basin, similar to those of the Athabasca Basin.

Note: References cited in poster are located in the accompanying digital file

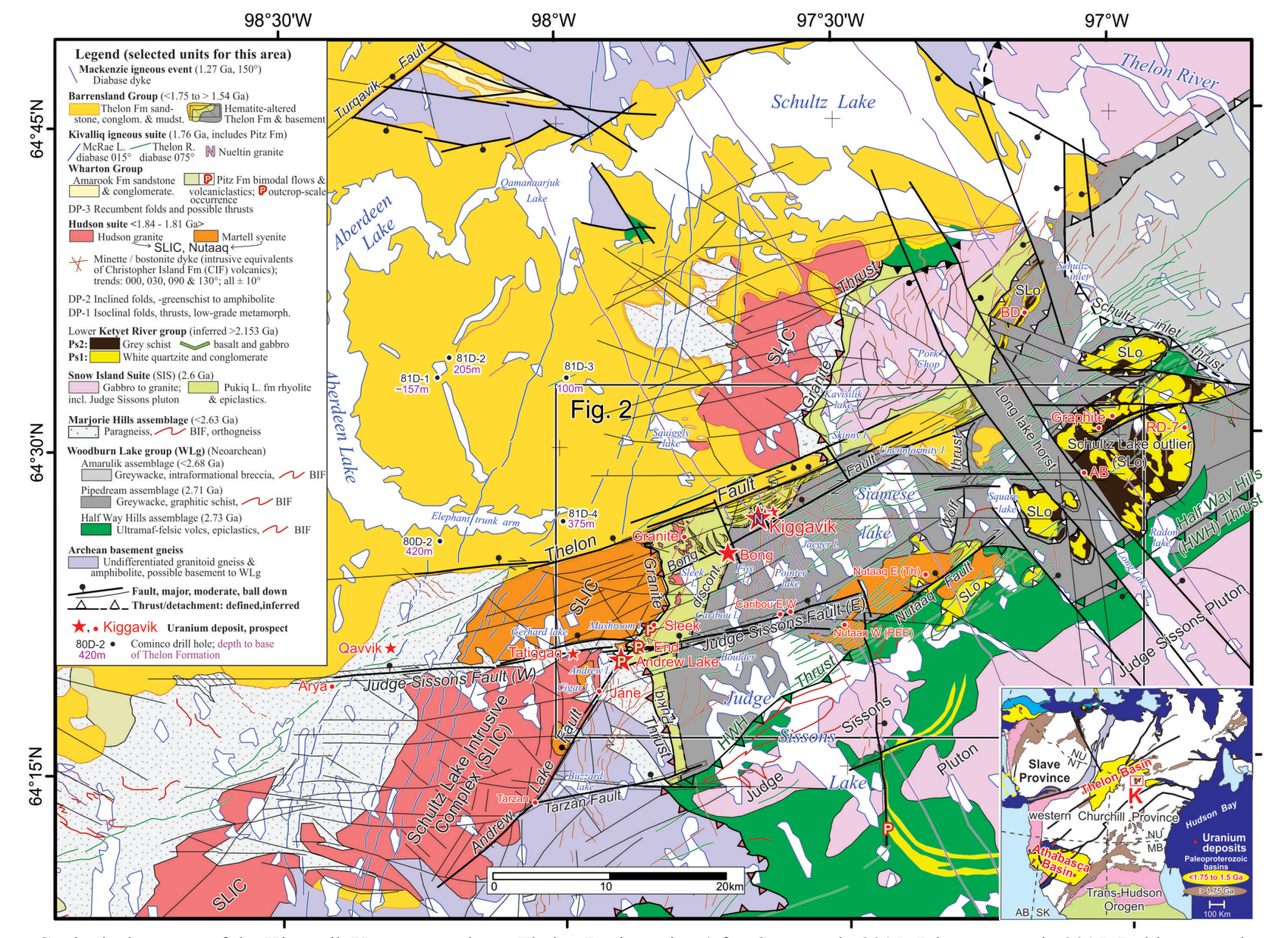

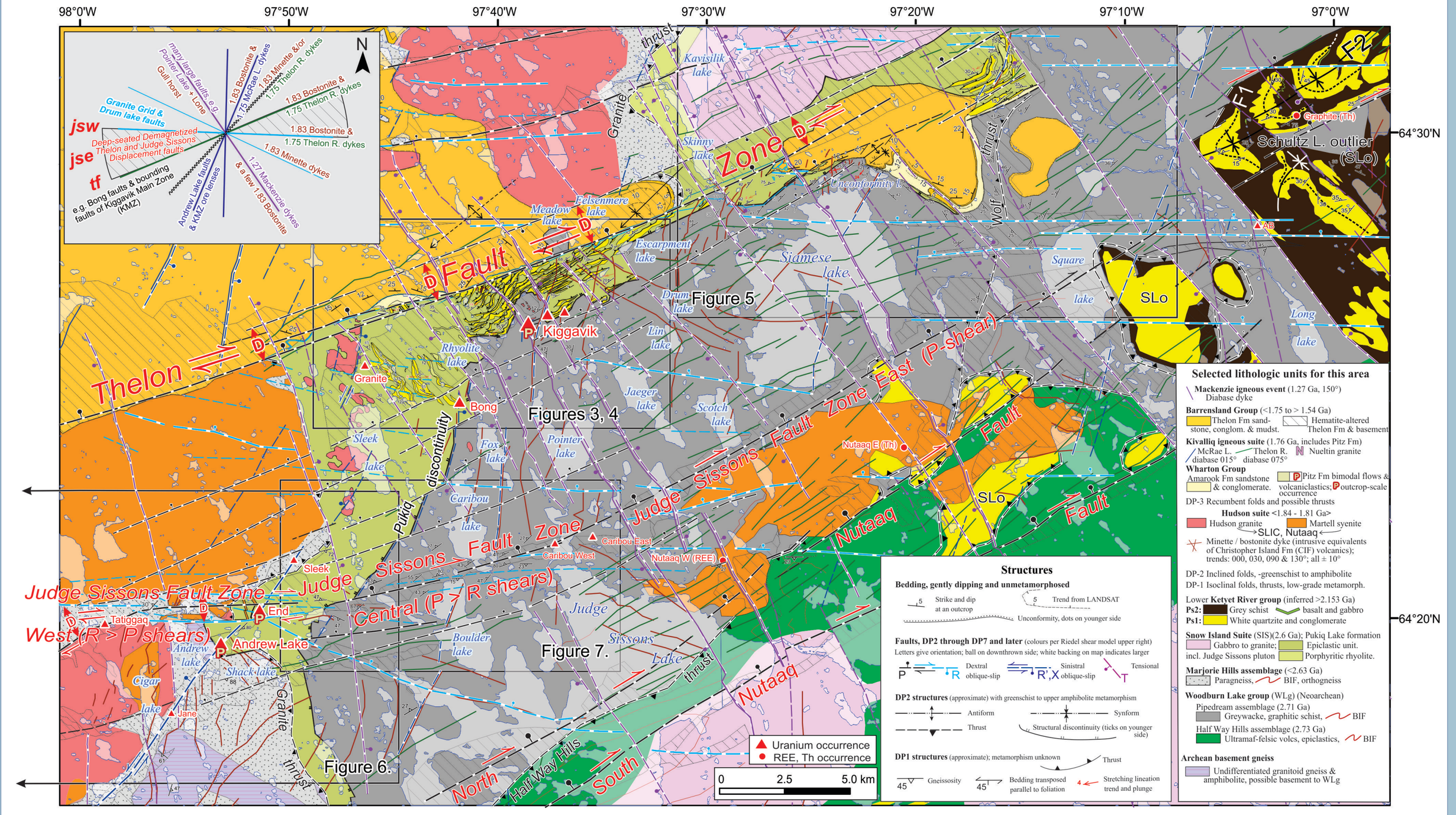

Figure 2A: Geology of Kiggavik U camp after Robinson et al. (2016), Johnstone et al. (2015). The "Hematite-altered Thelon Fm & basement" (hatched areas) outlines major negative aeromagnetic anomalies that transect other magnetic features and include intensely hematized outcrops, here interpreted as hydrothermal demagnetization along and extending laterally from reactivated fault zones, after Riegler (2013) and Riegler et al. (2014). Black rectangles outline areas of detailed figures. Pukiq Lake fm (Fig. 1; Peterson et al. 2014) is here subdivided into epiclastic rocks (after Johnstone et al., 2015) and rhyolite. Only major faults shown. The orientations and locations of dyke swarms correlate spatially with minor faults shown in Figure 2B which covers the same area. Data are insufficient to resolve the moderately dipping to sub-horizontal imbricate rhyolite-epiclastic-quartzite structures in the Bong to Granite Grid area, due in part to poor outcrop and evidence of later folding. Research by Dillon Johnstone (pers. com. 2016) aims to resolve them.

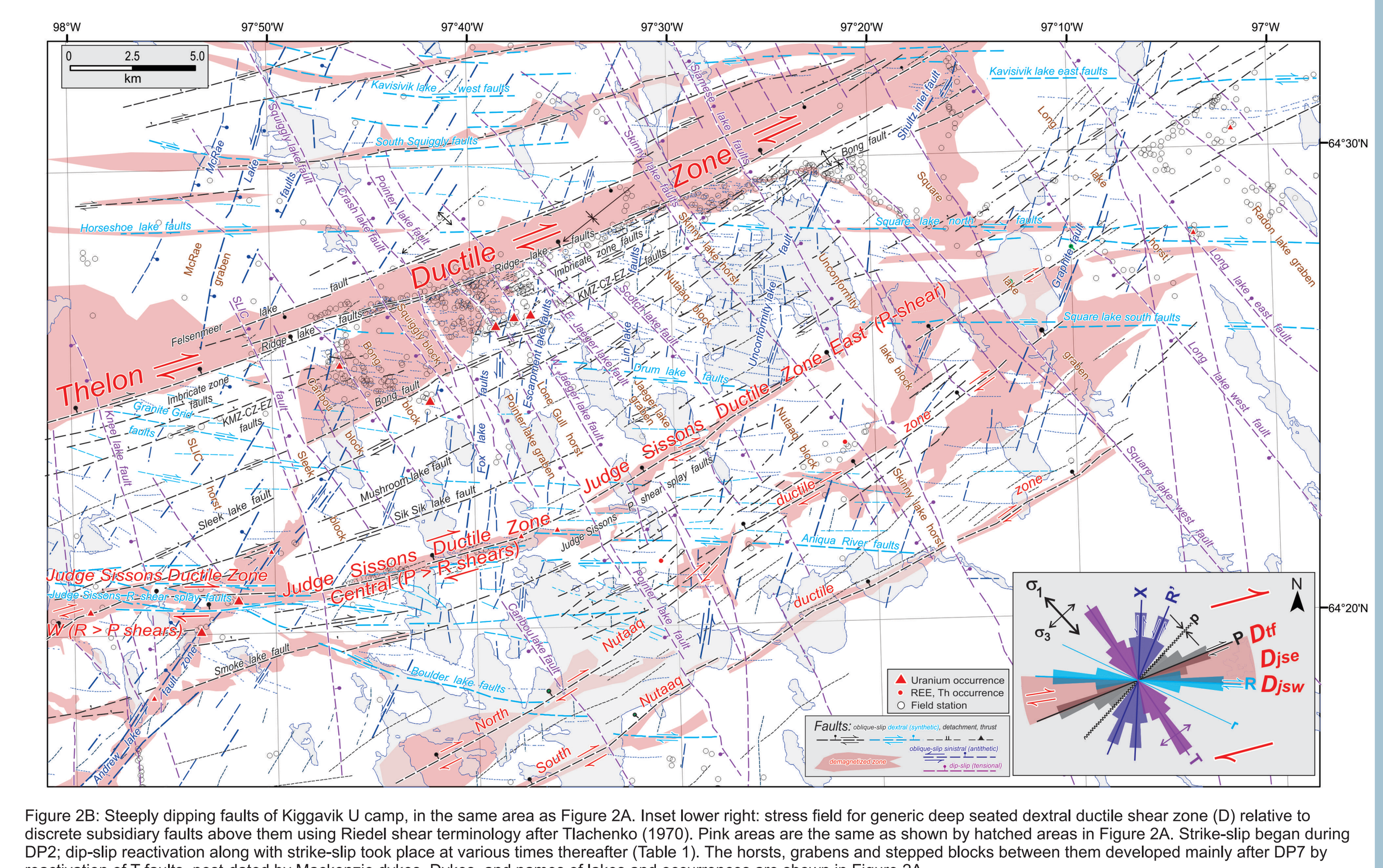

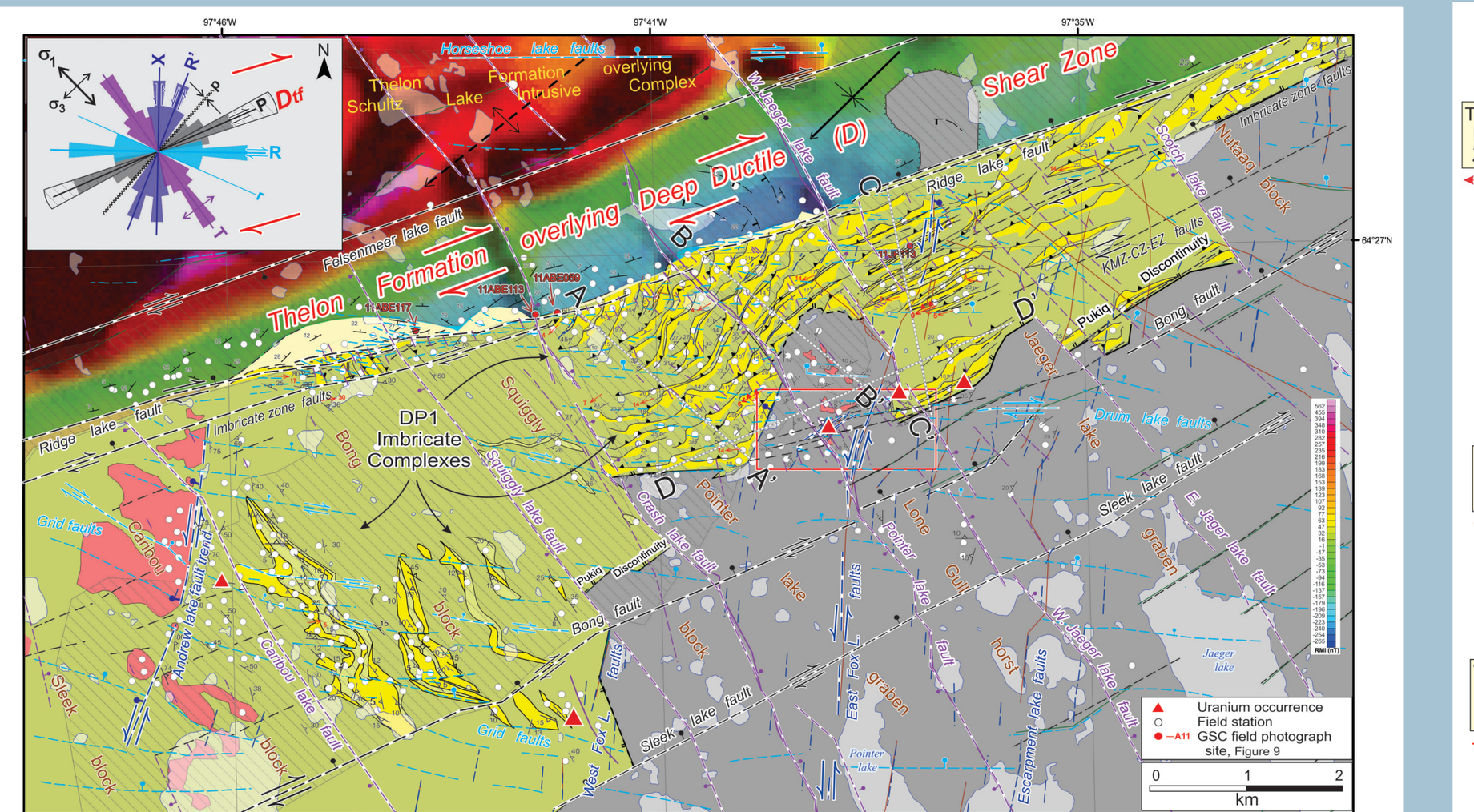

Table 1. Correlation of structural, depositional, magmatic & alteration events in the NE Thelon Basin region (after Jefferson et al. 2015).

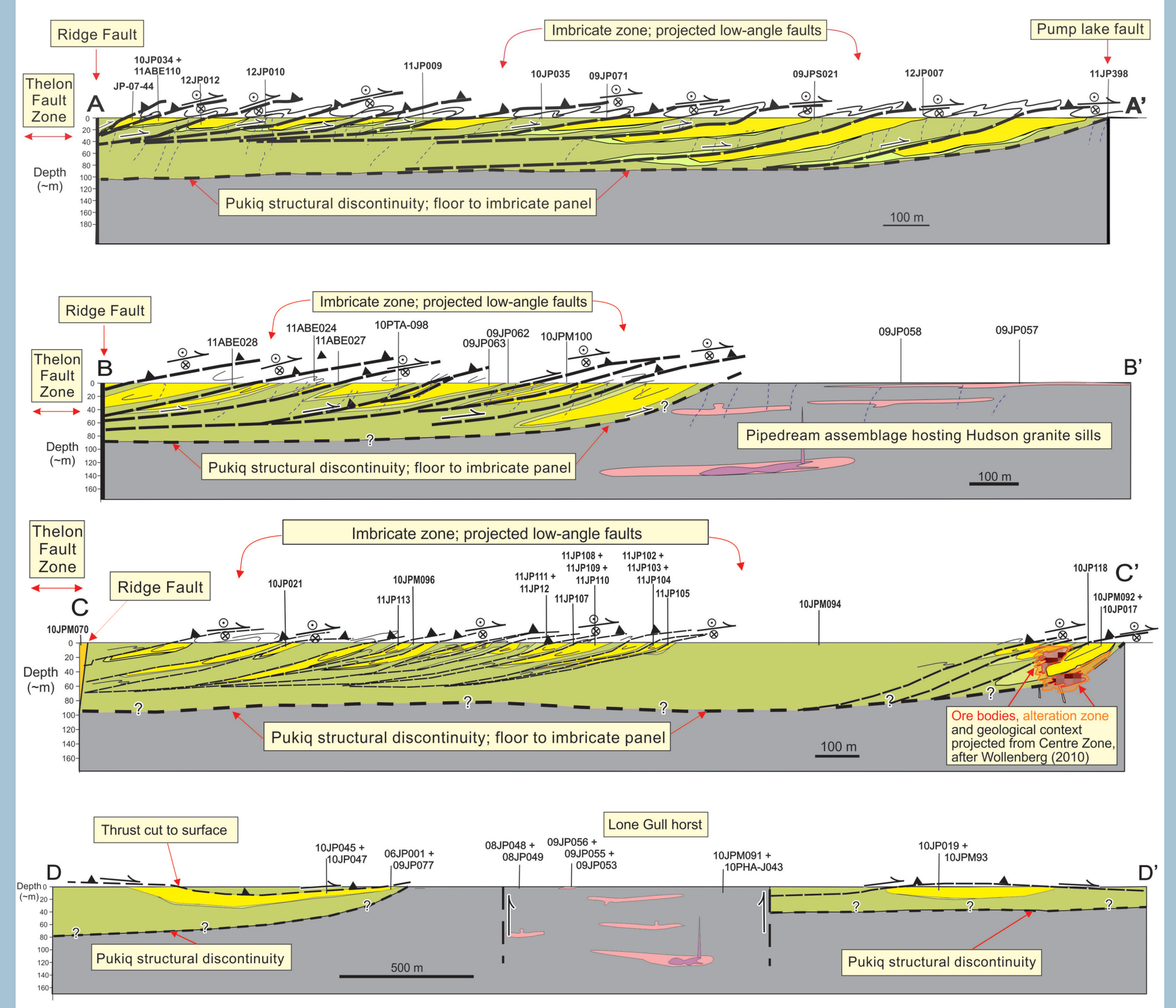

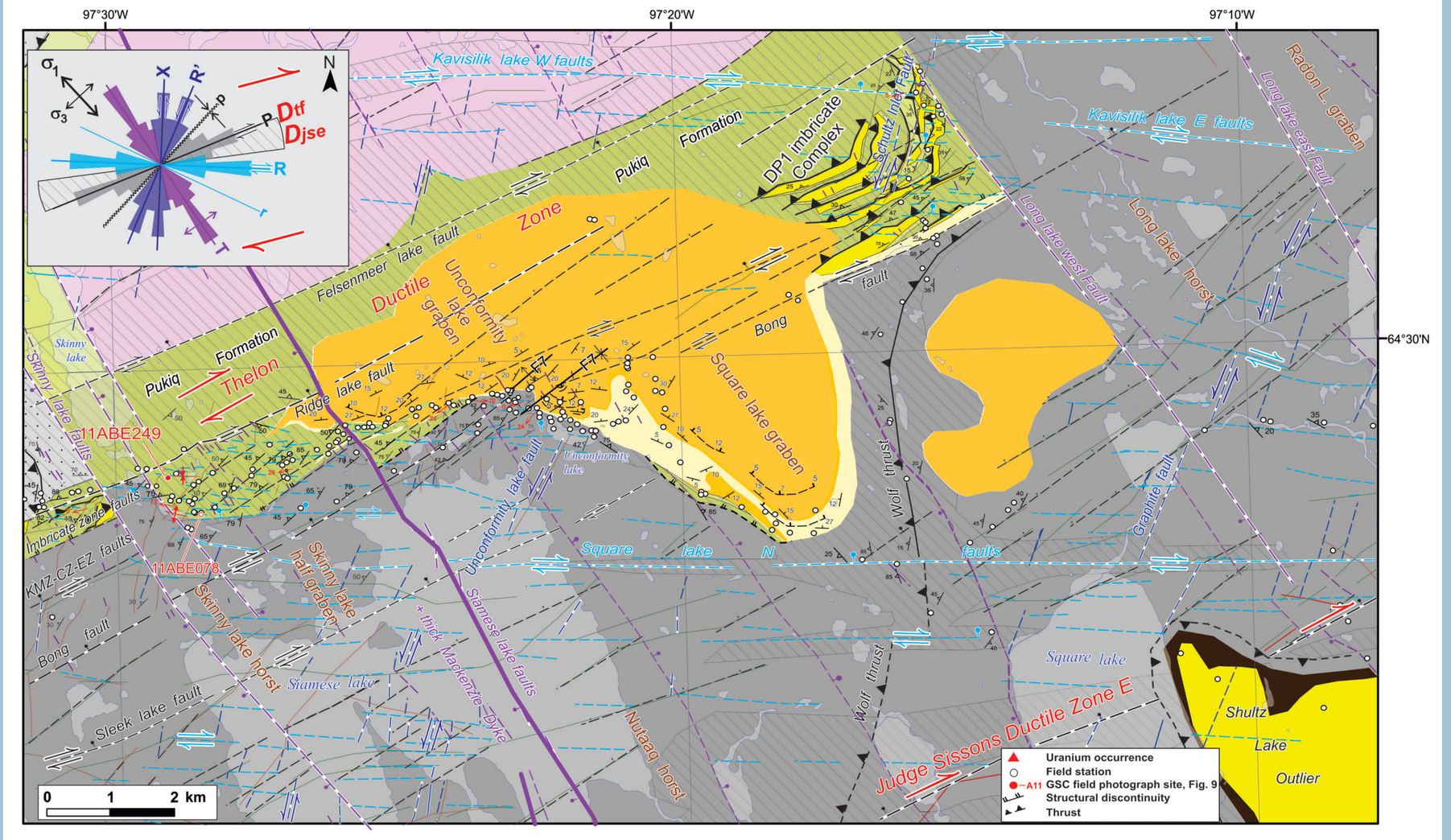

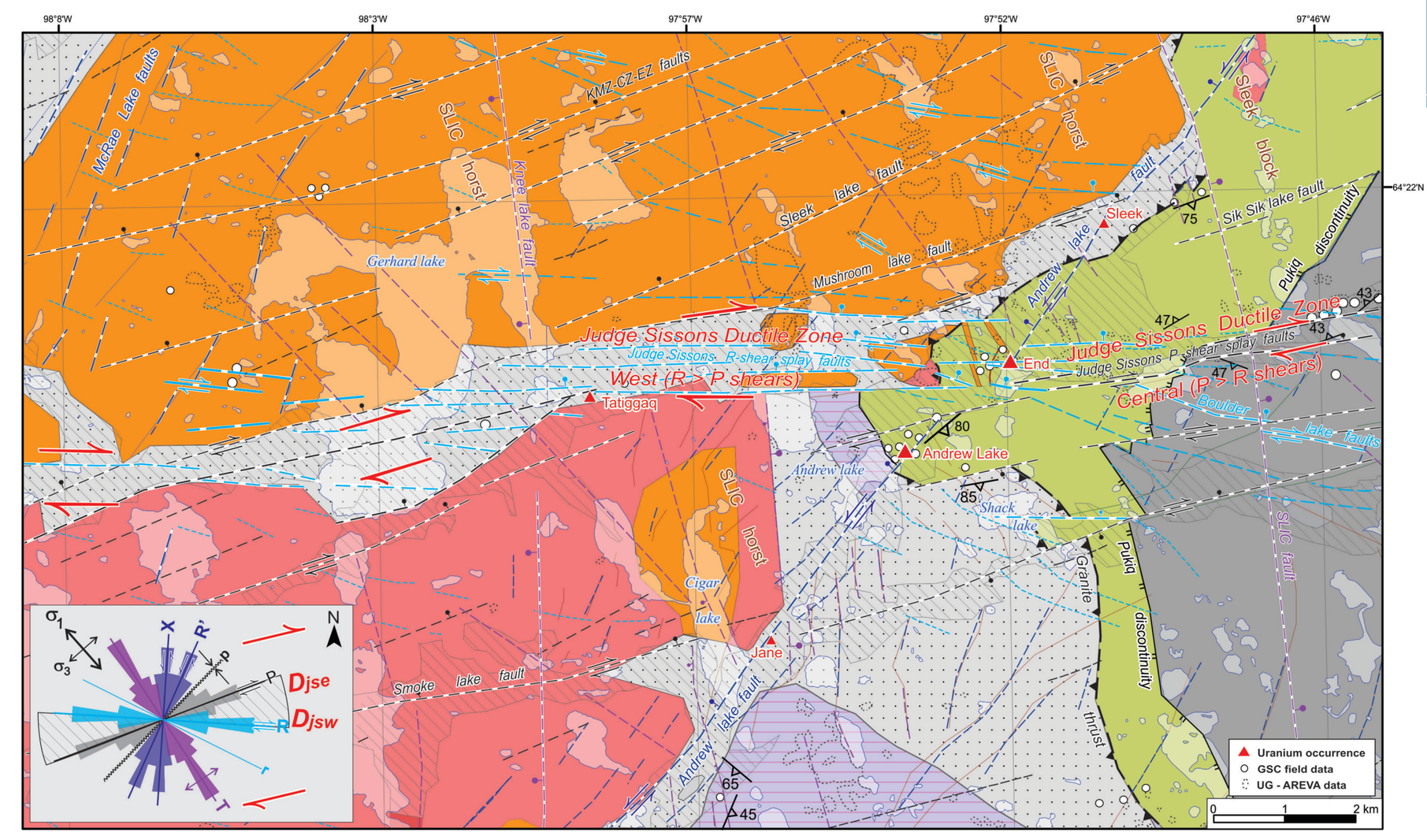

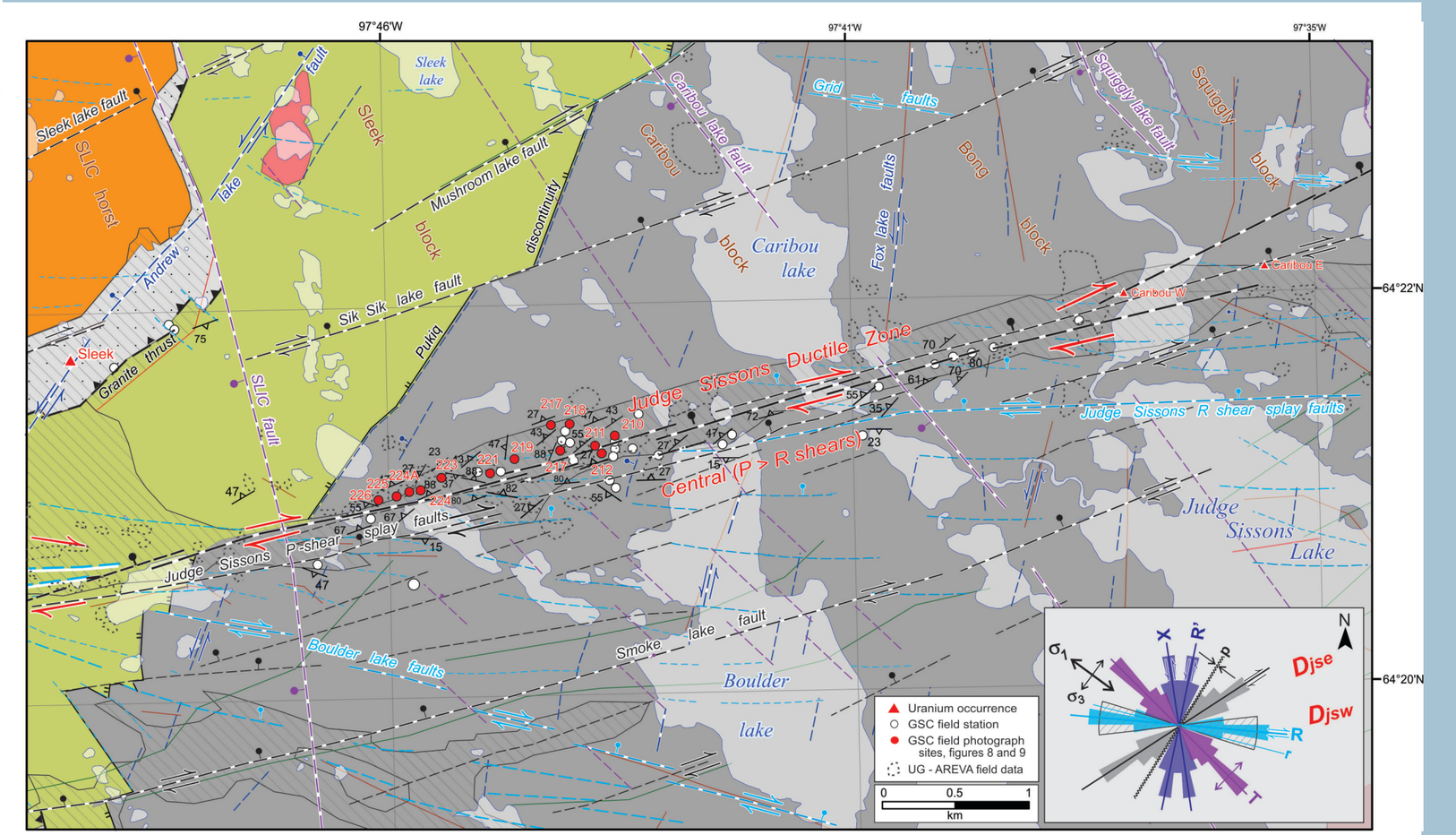

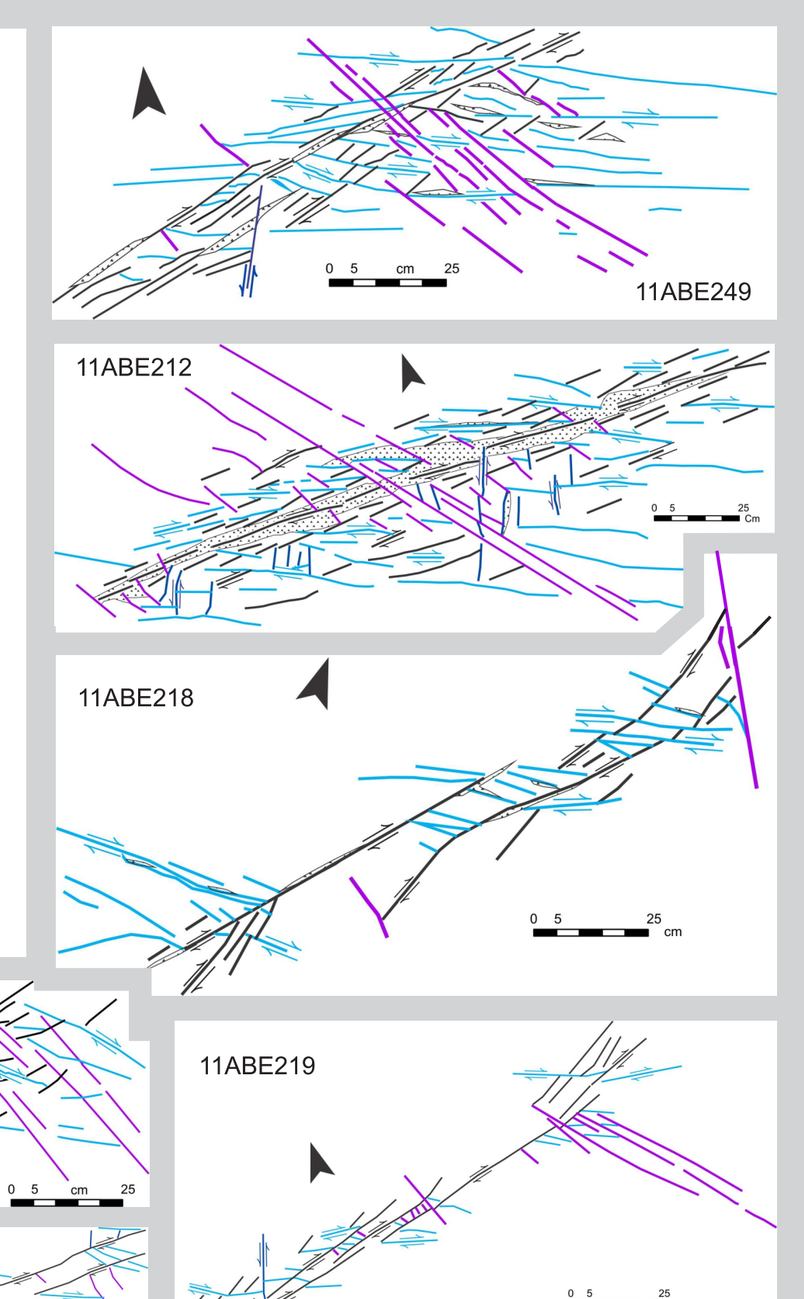

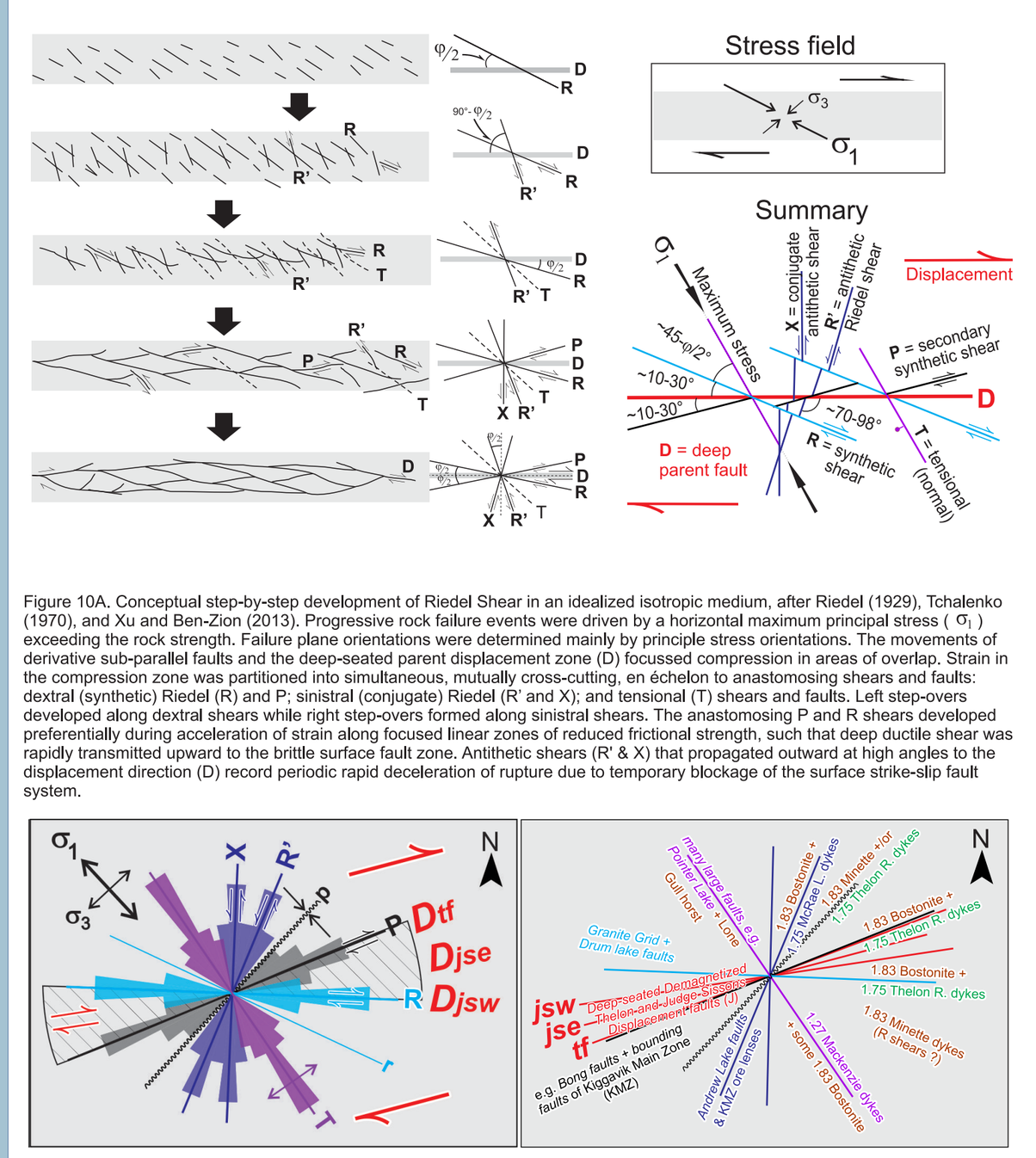

Figure 10B. Left: summary terminology adapted from 10A to respect observed angular relationships and subjective frequency distribution (rose histogram) of Riedel shear components that are interpreted to have developed from overall dextral displacement during DP4 through DP7 in the Kiggavik uranium exploration camp. The component labels are explained in Figure 10A except for "p" that denotes pressure solution (Xu and Ben-Zion, 2013). Deep displacement codes are: Dtf = Thelon Fault, Djsw = western Judge Sissons Fault, Djse = eastern Judge Sissons Fault. The observational data include faults, fractures and dykes mapped at various scales in outcrop (examples in Figure 9), aeromagnetic and LANDSAT lineaments (Anand and Jefferson, 2017), and geochronology (V. McNicoll, unpublished data and Jefferson et al., 2015).

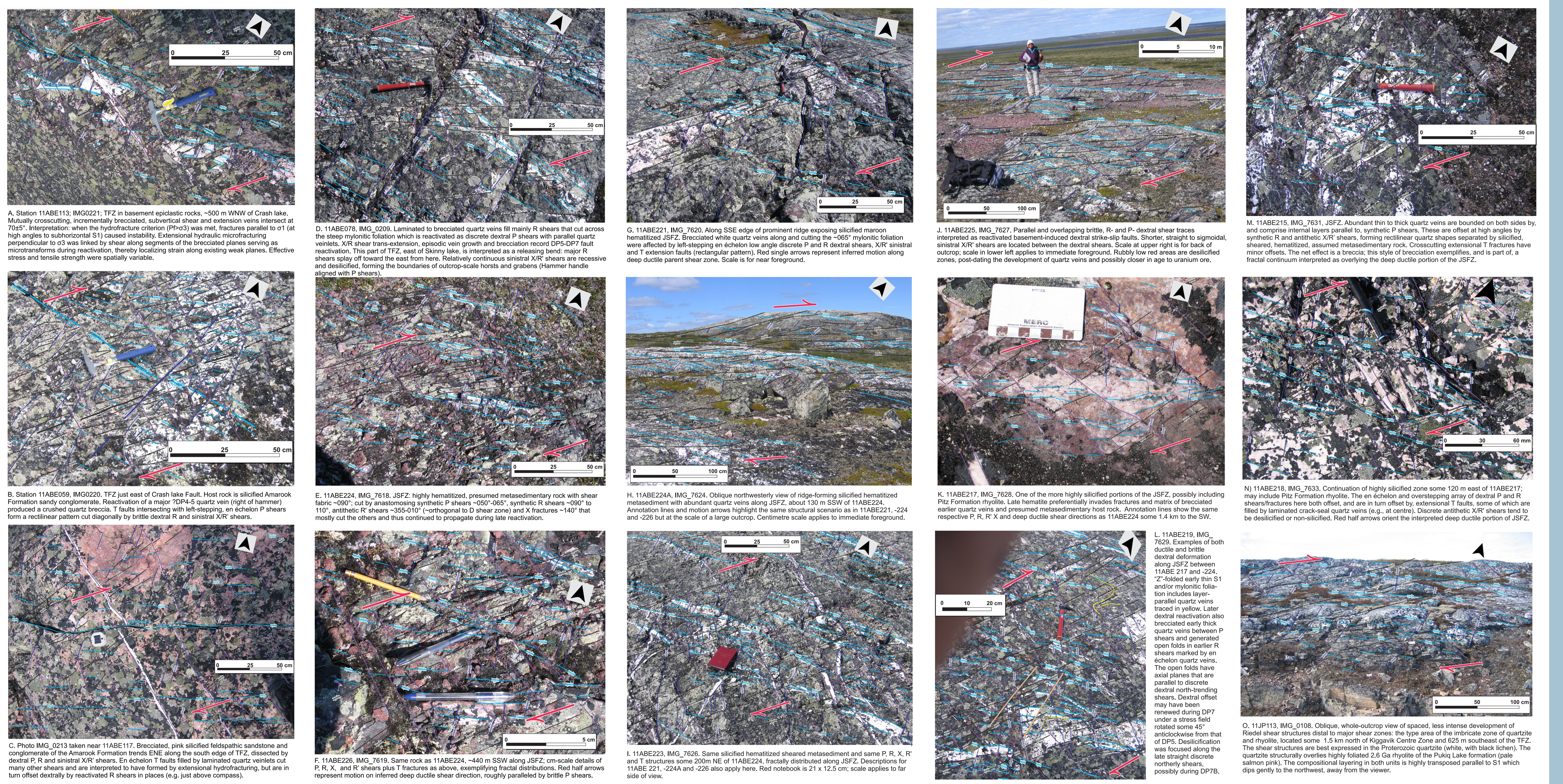

C. Photo IMG_0213 taken near 11ABE117. Brecciated, pink silicified feldspathic sandstone and conglomerate of the Amarook Formation trends ENE along the south edge of TFZ, dissected by dextral P, R and sinistral X/R' shears. En échelon T faults filled by laminated quartz veinlets cut many other shears and are interpreted to have formed by extensional hydrofracturing, but are in turn offset dextrally by reactivated R shears in places (e.g. just above compass).

F. 11ABE226, IMG_7619. Same rock as 11ABE224, ~440 m SSW along JSFZ; cm-scale details of P, R, X, and R' shears plus T fractures as above, exemplifying fractal distributions. Red half arrows represent motion on inferred deep ductile shear direction, roughly paralleled by brittle P shears.

I. 11ABE223, IMG_7626. Same silicified hematitized sheared metasediment and same P, R, X, R' and T structures some 200m NE of 11ABE224, fractally distributed along JSFZ. Descriptions for 11ABE 221, -224A and -226 also apply here. Red notebook is 21 x 12.5 cm; scale applies to far side of view.

Introduction

This report documents basement structures relevant to unconformity U deposits in the Kiggavik camp (Figure 1). Anand and Jefferson (2017) regionally mapped lineaments that are here interpreted as deep ductile to reactivated brittle-ductile surface faults (Fig. 1, 2A, Table 1) developed during DP2 (~1.83 Ga) through DP7 (~1.67 Ga) by Riedel shear (Riedel, 1929; inset A of figure 2B). Here we document Riedel shear structures in outcrop, their effects upon imbricated Paleoproterozoic quartzite, 2.6 Ga volcanic rocks and underlying 2.71 Ga metagreywacke, and discuss these relationships with respect to uranium deposits.

Acknowledgments

Considerable data, conceptual inputs and logistical support from industry partners, academic and fellow GSC collaborators and support staff, and local businesses are acknowledged in detail by Anand and Jefferson (2017). Our distribution of the epiclastic member of the Pukiq Lake formation from Bong through Kiggavik was influenced by Johnstone et al. (2015, 2016) who has characterized and greatly extended our knowledge thereof. Insightful critical reviews by Dr. K. Bethune and D. Johnstone (U. of Regina) were most helpful, as were comprehensive scientific editing and input from D. Lemkow (GSC).

Poster layout and associated data release

This camp-scale structural analysis considers detailed outcrop maps, structural measurements and field sketches for selected stations along the Thelon and Judge Sissons fault zones. Figures 2A and 2B provide geological and structural frameworks respectively, names used throughout, and locations of detailed maps. The Thelon Fault Zone is re-defined as a demagnetized deep ductile zone mainly covered by a 2 km-wide synclinal finger of Thelon Formation, bounded by the shallow Ridge lake (formerly named Thelon Fault) and Felsenmeer faults. The Bong to Kiggavik area (Figure 3) exemplifies intersections between the shallowly dipping imbricate complex and steeply dipping fault arrays. Schematic cross sections (Figure 4) illustrate the pre-DP2 configuration of the imbricate complex. Figures 5 to 9 document selected outcrop data on the strike- and dip-slip fault networks that dissected the imbricate complex and other parts of the study area (see Discussion for possible relevance to mineralization). Figure 10 shows how these data fit the Riedel shear model. Elements of each fault array have various dips, therefore rather than following the right hand rule, directions are labelled as in the NE or SE quadrants. Figure 11 places work by Fuchs and Hilger (1989) into this context. References and figures are included in the accompanying digital files. Individual field station data and ArcGIS geology shapefiles will be published in Jefferson et al. (*in prep. a, b*).

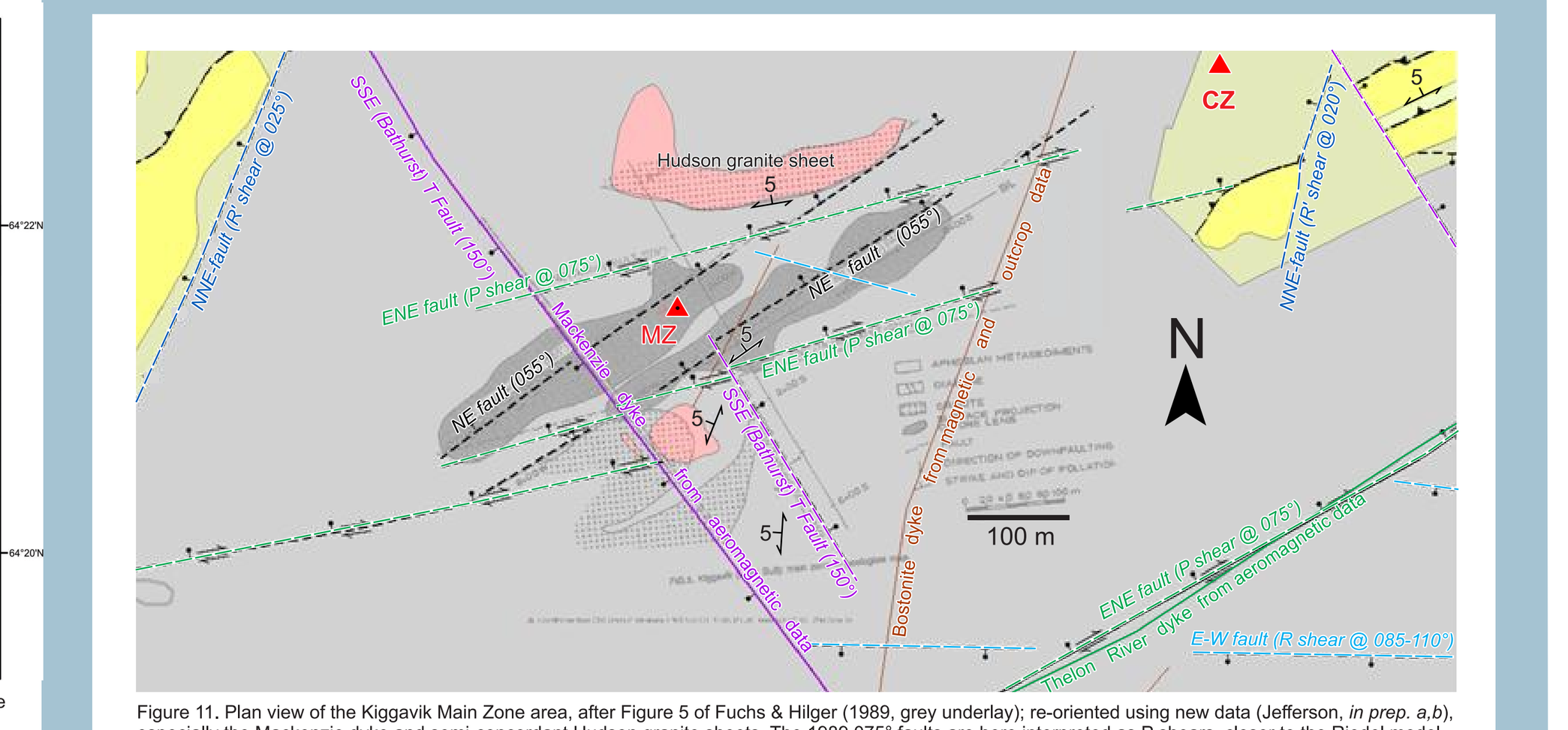

Discussion and Questions for the Future

Faults mapped at surface are relevant to the location and development of unconformity-associated uranium ore deposits in multiple, yet indirect and conceptual ways. The study area was subject to repeated anisotropic deformation from at least 1.83 Ga to the post-Ordovician (Table 1). Reactivated faults, key for unconformity U deposits (Jefferson et al., 2007a, b, c), have long been recognized in this region (e.g. Fuchs et al., 1986; Fuchs and Hilger, 1989; Hunter et al., 2012, 2014, 2015; Jefferson et al., 2011a, b; Miller and LeCheminant, 1985; Miller and Peterson, 2015). Second, the stress regime changed with, and/or between, each deformation event (codes in Table 1). Third, metallogenic studies cited above and in Table 1 have shown that different types of alteration and mineralization are linked to each deformation and magmatic event. Such linkages suggest age constraints on the various styles of steeply dipping structures pervading the Kiggavik Camp.

Many of the fault zones and adjacent rocks are altered by pervasive hematite and quartz cement and cut by numerous cross-cutting quartz veins and veinlets (Fig. 9). Both veins and cement comprise drusy and cryptocrystalline quartz such as documented by Turner et al. (2001) at Mallery Lake. We interpret the silicification as part of event DP5C that Peterson et al. (2014, 2015) link with heating during the Kivalliq Igneous Event. The relatively early nature of most quartz veins is consistent with observations by AREVA that much of the silicification and quartz veins predate de-quartzification and clay alteration associated with uranium mineralization (Riegler, 2013; Riegler et al., 2014; Sharpe et al., 2015). Nonetheless multiple generations of quartz veins (Fig. 9) and quartz cement in the Thelon Formation allow that some quartz veins may be contemporaneous with ore, accepting distal silica from de-quartzification and silicate alteration at the site of uranium precipitation.

Most of the fault zones that were silicified during DP5C were selectively de-quartzified during mineralization which, through regional metallogenic context, we ascribe to DP7A through DP7B. We have insufficient information to define the exact stress regime during mineralization, but uraninite is intergrown on a sub-microscopic scale with felted clay minerals that fill millimetre-scale veinlets; and clay mineral foliations form strain shadows around uranium-bearing fluorapatite crystals that are replaced by uraninite (Robinson et al., 2016). Spatial geometric analysis of such fabrics in oriented core samples could provide information to better understand deformation during mineralization.

Regardless of the timing of fault reactivation and reorientation of the stress field, several empirically mappable structural features likely influenced the paths of hydrothermal fluids that dissolved quartz, altered mafic minerals to hematite and clays, and precipitated uraninite in favourable sites. One large factor is the aquitard effect of the imbricate complex that may have formed a cap over hydrothermal fluid flow systems and thereby promoted lateral flow. The imbricated complex of quartzite, rhyolite and epiclastic rock (Fig. 3, 4, 7) is interpreted as a result of isoclinal folding and thrusting during DP1 (Table 1). Thin-skinned thrust imbrication within the complex records various states of internal plastic deformation, refolding and structural intercalation along lithologic contacts down to the millimetre scale. This imbricate panel dips gently to the NNW and is thought to have been an aquitard that was breached by the steeply dipping arrays of Riedel shears, somewhat along the length of some shears and especially where they branch, step and intersect with other contemporaneous structures. Some compressional clay-filled shears may have been aquitards that cut off fluid flow while intersecting extensional structures may have enhanced fluid flow, as suggested by Figure 11.

Multiple lines of evidence show that repeated reactivation through time generated strain along previously established zones of weakness rather than along ideal planes of an homogeneous model. Timing is provided by the above-noted alteration types and by dykes (Fig. 1, 2A) whose magnetic lineaments were used by Anand and Jefferson (2017) as evidence for faults and fractures with respect to the stress model (Fig. 9). The 1.83 Ga minette and bostonite dykes fill all fracture orientations of the stress model. Of the 1.75 Ga dykes, the McRae Lake dykes occupy only R' shears, only west of the SLIC. The Thelon River dykes fill both P and R shears. The 1.27 Ga Mackenzie diabase dykes fill only X faults and, in many places, cross over and are beside the most significant X faults, clearly post-dating ore-related faulting.

Brittle surface structures were mapped along the 1-3 km wide, broadly demagnetized deep crustal ductile shear zones (D) of Tschirhart et al. (2013a, b) and Anand and Jefferson (2017) (pink in Fig. 2B). The Thelon and Judge Sissons faults offset the SLIC by 25 and 10 km, respectively. The Andrew Lake fault is a large R' structure with little apparent sinistral offset. Renewed dextral offset along Thelon Fault offset the 1.75 Ga McRae Lake dykes by a few 10's of m. The recessive, broad, desilicified, demagnetized fault zones are mostly covered: Thelon by a finger of Thelon Formation; Judge Sissons and Andrew Lake by till. Their margins were reactivated as narrow, discrete but still complex fault and breccia zones some 10's to 100's of metres wide. Late slickensides on the Ridge lake fault (southernmost strand of the Thelon Fault) record north-down motion, consistent with drilled offsets of 100's of metres (Davis et al., 2011). The brittle surface structures predictably follow Riedel (R and R'), P and X shears. En échelon dextral R shears strike ~17° to 28° clockwise to D. En échelon dextral P shears strike ~10-15° anticlockwise of D. These are linked into continuous anastomosing fault zones parallel to D. Between the D zones discrete medium-scale faults (Fig. 2B) are spaced some 2 km apart and also record strike-, then dip-slip offsets shown by north-down steps in magnetic intensity. Scales range down to microscopic in a fractal continuum, including block to grain rotation and formation of breccia to cataclasite along all orientations, contained within much less deformed zones. Faults decrease laterally away from intense zones, grading into relatively unfractured rock. All shear orientations cut all others from place to place.

The ductile-brittle to brittle Riedel, P and X structures (Figure 10) fit classic definitions by Riedel (1929), Tchalenko (1970), Wilcox et al. (1973), Rutter et al. (1986), Davis et al. (1999), Nova (2003), Schmocker et al. (2003) and Xu and Ben-Zion (2013); experimental results simulating primary and reactivated deformation (Cloos 1928; Riedel 1929; Tchalenko 1970); field studies (e.g. Moore 1979; Davis et al. 1999; Ahlgren 2001; Katz et al. 2004); analogue modelling with clay (e.g. Cloos 1955; Wilcox et al. 1973; Tchalenko 1968; Smith and Durney 1992; Marques 2001) and sand (e.g. Naylor et al. 1986); direct shear experiments (e.g. Bartlett et al. 1981; Moore and Byerlee 1992; Schreus 1994) and numerical modelling (e.g. Dresen 1991; Braun 1994; McKinnon and Garrido de la Barra 1998).

Many structural questions remain. Regional DP2 transpression generated dextral shear zones, open to tight box folds broken by reverse faults and thrusts. The Schultz Lake outlier (Fig. 2) may be a klippe (Hadlari et al. 2004, Tschirhart et al. 2013a, McEwan 2012) but more work is needed along its margins. Late in DP2 to DP3 trans-extension exhumed the 1.83 Ga Hudson suite. Extension along the Wharton Lake fault system west of Kiggavik and major faults to the southeast accommodated the Baker Lake Group. Extension also generated F3 folds with subhorizontal axes and drove retrograde metamorphism. Questions abound regarding the inferred Pukiq Lake discontinuity - we prefer a DP3 and/or younger extensional structure but it could be a highly strained unconformity surface between the younger Pukiq Lake formation and older Pipedream assemblage. Reversed strike slip motion along some P and R shear faults has yet to be explained. Renewed transpression during DP4 reactivated the long-lived, deep and pervasive, ductile dextral strike-slip systems from DP2 and developed proximal ENE-trending folds and thrusts. How important are DP4 folds measured at Granite Grid and just north of the Lone Gull camp for constraining ore? Which brittle-ductile to late brittle DP4 faults reactivated weaknesses from previous deformations, and which are new? During DP5, 6 and 7 successive dextral trans-extension events accommodated the Wharton and Barrensland groups, punctuated by erosion during quiescence and uplift. Do the Figure 11 structures documented by Fuchs and Hilger (1989) reflect DP5 to 7? What generation are their ore-constraining 055° faults and do they fit the Riedel shear model?

This Open File release is a product of Natural Resources Canada's Geo-mapping for Energy and Minerals (GEM) program.